APPLICATION OF A LABORATORY MICRO-X-RAY DIFFRACTOMETER (RIGAKU DMAX RAPID II) IN THE ARCHAEOMETRIC ANALYSIS OF ARCHAEOLOGICAL ARTEFACTS – CASE STUDIES OF METAL OBJECTS•

LABORATÓRIUMI MIKRO-RÖNTGENDIFFRAKTOMÉTER (RIGAKU DMAX RAPID II) ALKALMAZÁSA RÉGÉSZETI LELETEK ARCHEOMETRIAI VIZSGÁLATÁBAN FÉMTÁRGYAK PÉLDÁJÁN

MOZGAI, Viktória[1]; BAJNÓCZI, Bernadett[1]; MRÁV, Zsolt[2]; KOVACSÓCZY, Bernadett[3]; TÓTH, Mária[1]

[1]Institute for Geological and Geochemical Research, Research Centre for Astronomy and Earth Sciences, Hungarian Academy of Sciences, H-1112 Budapest, Budaörsi út 45.

[2]Hungarian National Museum, H-1088 Budapest, Múzeum körút 14–16.

[3]Katona József Museum of Kecskemét, H-6000 Kecskemét, Bethlen körút 1.

E-mail: mozgai.viktoria@csfk.mta.hu

Abstract

X-ray diffraction (XRD) is a widely used method to specify the mineralogical composition of archaeological artefacts, e.g. the material of inlays or corrosion products of metal objects. Laboratory micro-XRD instruments, like the RIGAKU DMAX RAPID II micro-X-ray diffractometer (μ-XRD), can be used instead of conventional X-ray (powder) diffraction analysis if sampling is not or just limitedly allowed due to e.g. the high value of the archaeological object. In these cases, in situ non-destructive measurements directly on the object or on the detached, small-sized samples are preferred. The possible application of this laboratory micro-XRD instrument in the analysis of archaeological metal objects is demonstrated on the example of three case studies.

In order to reconstruct the manufacturing technique of Roman-period niello (black metal sulphide), niello inlays of a late Roman silver augur staff were analysed. Due to the uniqueness and high value of the well-dated and intact object, only non-destructive analytical methods were permitted. Based on the SEM-EDS and μ-XRD results, five niello types were found on the object: pure silver sulphide and different silver-copper sulphides (with silver/copper ratio from 3:1 to 1:1). The object was originally decorated with these diverse niello inlays indicating that silver-copper sulphide niello, even stromeyerite (AgCuS), was used by the Roman craftsmen two-hundred years earlier (last third of 3rd century AD) than the previous studies indicated (end of 5th century AD).

Corrosion products of a large-sized, late Roman copper cauldron were examined in order to characterise the burial environment. The corroded metal samples taken from the cauldron were analysed in cross section, layer-by-layer, using electron microprobe and μ-XRD analyses. Different corrosion products were identified: copper oxide (cuprite) and copper carbonate (malachite) are the products of passive corrosion indicating burial in a well-aerated, calcareous soil environment, whereas copper chloride (nantokite), copper hydrochloride (paratacamite/atacamite) and copper sulphate (brochantite) are the products of active corrosion forming after excavation.

Material and corrosion products of gold and gilded silver objects of the Hunnic Period were analysed by using electron microprobe and μ-XRD analyses. The surface of the high-purity gold objects is covered by a very thin reddish layer, which is a tarnish composed of mixture of gold-silver sulphide corrosion products. The silver objects were completely mineralised into silver sulphobromide and bromian silver chloride (embolite), typical corrosion products of silver alloys buried in soil environment (rich in organic matter). No copper corrosion products were detected indicating that the silver objects were most probably manufactured from high-purity silver alloy.

• How to cite this paper: MOZGAI, V., BAJNÓCZI, B., MRÁV, Zs., KOVACSÓCZY, B. & TÓTH, M., (2019): Application of a laboratory micro-X-ray diffractometer (RIGAKU DMAX RAPID II) in the archaeometric analysis of archaeological artefacts – case studies of metal objects, *Archeometriai Műhely* **XVI/1** 29-42.

Kivonat

A röntgendiffrakció (XRD) széles körben alkalmazott módszer régészeti leletek, pl. különböző berakások vagy korróziós termékek ásványos összetételének meghatározásában. Laboratóriumi mikro-XRD készülékek, mint a RIGAKU DMAX RAPID II mikro-röntgendiffraktométer (μ-XRD), jól használhatók a hagyományos, porpreparátumot igénylő röntgendiffraktométerek helyett, ha a mintavétel nem vagy csak korlátozott mértékben engedélyezett, például a régészeti tárgyak nagy értéke miatt. Ezekben az esetekben in situ roncsolásmentes méréseket részesítik előnyben közvetlenül a tárgyak felületén, vagy a kivett, kisméretű mintákon. A fent említett készülék régészeti fémtárgyak vizsgálatában való alkalmazhatóságát három esettanulmányban mutatjuk be.

A római korban alkalmazott nielló (fekete fém-szulfid berakás) készítéstechnikájának rekonstrukciójához egy késő római ezüst augurbot niellóberakásait elemeztük. A jól datált és érintetlen állapotban talált tárgy egyedisége és nagy értéke miatt csak roncsolásmentes vizsgálati módszereket alkalmazhattunk. A SEM-EDS és μ-XRD eredmények alapján a tárgyat ötféle niellóberakás díszíti: tiszta ezüst-szulfid és különböző ezüst-réz-szulfidok (ezüst/réz arány 3:1-től 1:1-ig). A tárgyat már a készítése során ezzel a változatos összetételű niellóberakással díszítették, ami arra utal, hogy már a római mesterek használták az ezüst-réz-szulfid niellót, még a stromeyeritet is (AgCuS), kétszáz évvel korábban (3. század utolsó harmada), mint ahogy a korábbi tanulmányok feltételezték (5. század vége).

Egy nagyméretű, késő római rézüst korróziós termékeit vizsgáltuk az eltemetési környezet jellemzéséhez. Az üstből levett korrodált rézmintákat keresztmetszetben, rétegről rétegre elemeztük elektron-mikroszondával és mikro-röntgendiffraktométerrel. Különböző korróziós termékeket különítettünk el: a réz-oxid (kuprit) és réz-karbonát (malachit) passzív korróziós termékek, amelyek jól átszellőzött, meszes talajkörnyezetben való eltemetés során alakultak ki, míg a réz-klorid (nantokit), réz-hidroklorid (paratacamit/atacamit) és réz-szulfát (brochantit) aktív korróziós termékek, amelyek a megtalálás után képződtek.

Hun kori arany- és aranyozott ezüsttárgyak anyagát és korróziós termékeit vizsgáltuk elektron-mikroszondával és mikro-röntgendiffraktométerrel. A nagy tisztaságú aranyból készült tárgyak felületét nagyon vékony vöröses bevonat borítja, ami korróziós termékek, arany-ezüst-szulfidok keverékéből álló réteg. Az ezüsttárgyak anyaga teljesen átalakult ezüst-szulfobromiddá és brómtartalmú ezüst-kloriddá (embolit), melyek (szerves anyagban gazdag) talajokban eltemetett ezüsttárgyak tipikus korróziós termékei. A rézkorróziós termékek hiánya arra utal, hogy a tárgyakat feltehetőleg nagy tisztaságú ezüstből készítették.

KEYWORDS: MICRO-X-RAY DIFFRACTION, NIELLO, CORROSION, SILVER, COPPER, GOLD

KULCSSZAVAK: MIKRO-RÖNTGENDIFFRAKCIÓ, NIELLÓ, KORRÓZIÓ, EZÜST, RÉZ, ARANY

Introduction

Material analysis of archaeological metal artefacts, especially their decorations, inlays or corrosion products, involves not only the study of microstructure and chemical composition, but in several cases the determination of mineralogical composition as well. X-ray diffraction (XRD) is a widely used method to specify the mineralogical composition (phase identification) of natural as well as artificial materials. However, when sampling is not or just limitedly allowed due to e.g. the high value of the archaeological object, the conventional X-ray diffraction analysis performed on powdered specimens can hardly be used. Laboratory micro-XRD instruments provide good alternatives, like the RIGAKU DMAX RAPID II micro-X-ray diffractometer (μ-XRD). One of the main advantages of laboratory μ-XRD over traditional (powder) XRD is its non-destructiveness (non-invasiveness). In most cases, no sampling or special specimen preparation is needed. Objects and small-sized, non-flat or non-smooth samples, in addition polished blocks and thin sections prepared for other, e.g. scanning electron microscope (SEM)/electron microprobe (EMP) and petrographic studies, can directly be analysed *in situ* without any further preparation. Besides non-destructiveness, with the RIGAKU DMAX RAPID II instrument an area as small as 10 μm in diameter can be analysed on the object/sample. However, some limits should be taken into consideration during data processing and evaluation. Due to the geometry of the instrument, the object/sample may cover certain areas of the imaging plate detector depending on its actual position in the diffraction geometry; therefore, some higher d_{hkl} values could not be detected. The areas, where measurements take place, neither are single crystals, nor represent an ideal powder. Measured peak intensities are increased or decreased in specific hkl crystallographic directions compared to that of powdered specimens due to preferred orientations; therefore, during data evaluation peak intensities cannot be taken into consideration, only peak positions are used. Another important issue is that the smaller collimator is used, the longer measurement time is needed in order to obtain adequate intensities.

The RIGAKU DMAX RAPID II micro-X-ray diffractometer has already been used in the archaeometric investigation of cultural heritage materials, e.g. mortars, glazes, glasses, pigments, stones (e.g. Benedetti et al. 2004; Bontempi et al. 2008; Swider 2010; Abbe et al. 2012; Kingery-Schwartz et al. 2013; Takumi & Maeyama 2015; Bajnóczi et al. 2016; Howe et al. 2018; Osváth et al. 2018). In this paper, we present three case studies showing how this laboratory micro-XRD instrument can be used in the investigation of archaeological (and historic) metal objects, where in most cases no or only very limited sampling is permitted due to the high value of the objects.

Methodology

Prior to micro-XRD analysis the microstructure and chemical composition of the analysed objects/samples were studied using a scanning electron microscope (SEM) or an electron microprobe (EMP).

A large chamber door (width 290 mm) AMRAY 1830i type scanning electron microscope equipped with EDAX PV 9800 energy-dispersive X-ray spectrometer (EDS) was used for large objects (*case study 1*). Analytical conditions: 20 kV acceleration voltage, 1 nA beam current, net counting time of 100 sec for the point and area analyses. The results were normalised to 100 wt%.

A JEOL Superprobe-733 type electron microprobe equipped with an Oxford Instruments INCA Energy 200 type energy-dispersive X-ray spectrometer (EDS) was used for small artefacts (maximum 5 cm in diameter, *case study 3*) or small-sized layered samples detached from corroded metal objects and embedded in epoxy resin (*case study 2*). Analytical conditions: 20 kV accelerating voltage, 6 nA beam current, 40–90 sec and 5–10 min acquisition time for point and area analyses, respectively. Natural and artificial materials of the Taylor Co. (Stanford, California) were used as standards during quantitative analyses, specifically gold (Au), chalcopyrite ($CuFeS_2$) and acanthite (Ag_2S) in *case study 3*. For considering sufficient amount of data, totals between 95 wt% and 105 wt% were evaluated (*case study 3*).

For the analysis of the largest buckle in *case study 3*, a ZEISS EVO 40XVP scanning electron microscope equipped with Oxford Instruments INCA ISIS energy-dispersive spectrometer (EDS) was used. Analytical conditions: 20 kV accelerating voltage, 6 nA beam current and 30 sec acquisition time. The results were normalised to 100 wt%.

The mineralogical composition of the samples presumed on account of the SEM-EDS/EPMA results was verified with the use of RIGAKU D/MAX RAPID II micro-X-ray diffractometer (μ-XRD), which is a unique combination of a MicroMax-003 third generation microfocus, sealed tube X-ray generator and a curved imaging plate detector (**Fig. 1a**, for analytical conditions in each case study see **Table 1.**). The diffractometer was operated with CuKα radiation generated at 50 kV and 0.6 mA. Different types of collimators can be used (10 μm, 30 μm, 50 μm, 100 μm, 300 μm, 500 μm, 800 μm) depending on the size of the measured area. A built-in CCD camera was used to select the measurement areas. A laser scanning readout system reads the imaging plate detector in about 1 min. RIGAKU 2D Data Processing software 2DP was used to record the diffraction image from the laser readout. For each XRD pattern the interpretable 2Θ region was selected manually. RIGAKU PDXL 1.8 integrated X-ray powder diffraction software was used for data processing.

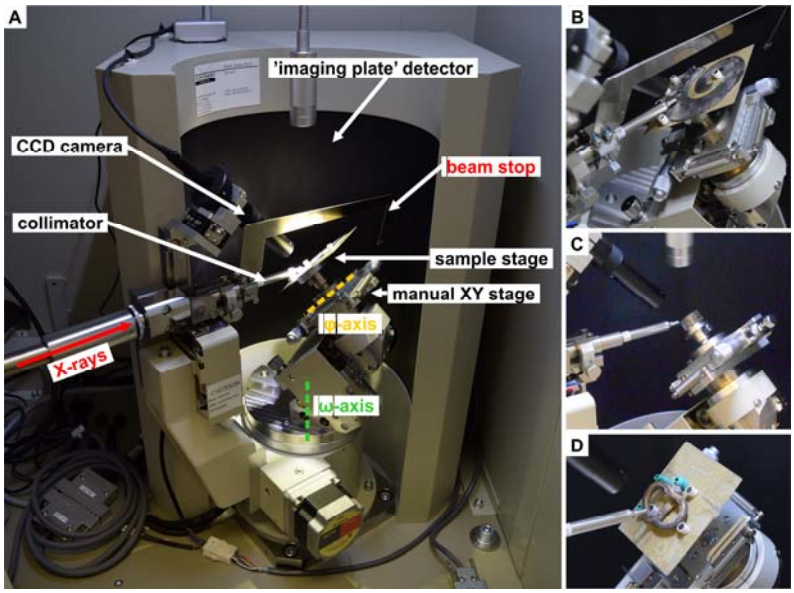

Fig. 1.:

A: The setup of the RIGAKU DMAX RAPID II micro-X-ray diffractometer. B–D: objects/samples of the case studies mounted onto the sample holder.

1. ábra:

A: A RIGAKU DMAX RAPID II mikro-röntgendiffraktométer felépítése. B–D: az esettanulmányokban vizsgált tárgyak/minták elhelyezkedése a mintatartón.

Table 1.: Analytical conditions of μ-XRD measurements in the case studies discussed in the paper

1. táblázat: A három esettanulmány μ-XRD vizsgálatainak mérési körülményei

	CASE STUDY 1	CASE STUDY 2	CASE STUDY 3
Sample preparation	-	polished cross sections	-
Collimator	100 μm	10–100 μm	50–800 μm
Measurement time	5–20 min	10–40 min	1–60 min
ω-axis	20–30°	0–25°	0–35°
φ-axis	0–25°	20–115°	0–15°

Case study 1: Niello inlays of a late Roman silver augur staff

Niello is a bluish black inlaying material, which was widely used to decorate metal objects from the 1st century AD and is still used today. Its composition has changed through times depending on the metal it decorates. As no written sources are available for niello manufacturing from the Roman period, our knowledge about the contemporary technique is very sparse. Based on previous studies, it has been widely accepted that Roman niello was generally composed of one metal sulphide, the same as it decorates e.g. silver sulphide (acanthite, Ag_2S) was used for silver objects (Moss 1953; Dennis 1979; Newman et al. 1982; La Niece 1983; Oddy et al. 1983; Schweizer 1993; Northover & La Niece 2009). Binary silver-copper sulphide niello (stromeyerite, AgCuS) was apparently used intentionally only from the end of 5th century AD (Dennis 1979; Newman et al. 1982; La Niece 1983; Oddy et al. 1983; Schweizer 1993; Northover & La Niece 2009).

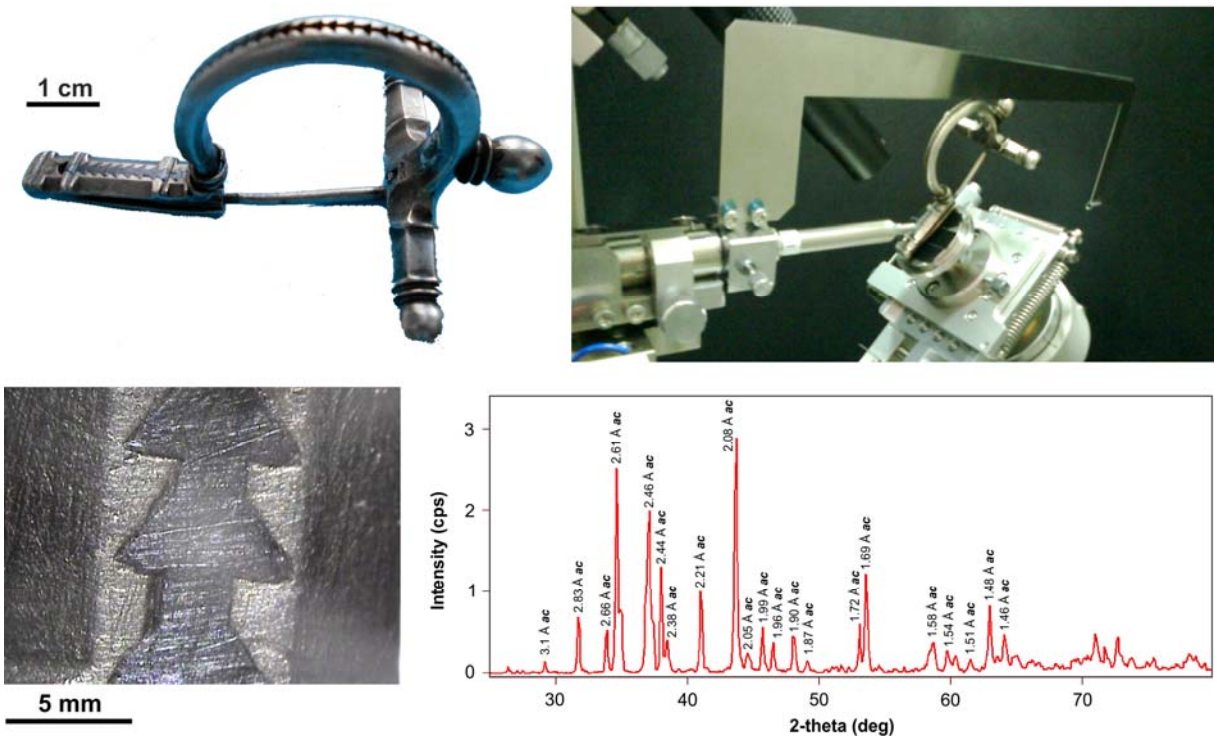

Fig. 2.: A late Roman niello-inlaid silver fibula (photo: A. Dabasi, Hungarian National Museum) and its position in the micro-X-ray diffractometer. Binocular microscopic image and μ-XRD pattern of the niello inlay of the fibula. Abbreviation: ac = acanthite (Ag_2S) (PDF 00-014-0072).

2. ábra: Késő római niellóberakásos ezüstfibula (fotó: Dabasi A., Magyar Nemzeti Múzeum) és rögzítése a mikro-röntgendiffraktométerben. A niellóberakás sztereomikroszkópos képe és diffraktogramja. Rövidítés: ac = akantit (Ag_2S) (PDF 00-014-0072).

In order to better understand the late Roman niello technique, several niello-inlayed objects (Mráv 2010a, 2010b, 2011), found in the Pannonian provinces and preserved now in the Hungarian National Museum, were analysed by using handheld X-ray fluorescence spectrometry (hXRF) and proton-induced X-ray emission spectrometry (PIXE) (Mozgai et al. 2016). Most of the analysed objects was decorated with one metal sulphide niello confirming the previous studies, as in the case of a silver fibula dated to the second half of the 3rd century, for which micro-XRD measurements verified the only presence of silver sulphide (acanthite, Ag_2S) (**Fig. 2.**). However, the niello inlays of a silver augur staff (*lituus*) (**Fig. 3.**) showed elevated and inhomogeneous copper content (up to 30 wt% based on PIXE analysis). The object was excavated from an undisturbed grave in *Brigetio* (Komárom-Szőny in Hungary) in the 1960s and it is the only known silver augur staff from the territory of the Roman Empire (Barkóczi 1965, Tóth 2017). A more detailed examination regarding the microstructure and the mineralogical composition of niello inlays was performed non-destructively due to the high value of the object by using SEM-EDS and μ-XRD (**Fig. 1b**).

Five niello types were identified, their chemical compositions range from silver sulphide (acanthite) to binary silver-copper sulphide of Ag:Cu ratio 1:1 (stromeyerite). Type 1 niello is homogeneous polycrystalline silver sulphide (acanthite, Ag_2S); Type 2 niello is inhomogeneous silver-copper sulphide (exsolution of acanthite, Ag_2S and jalpaite, Ag_3CuS_2); Type 3 niello is homogeneous polycrystalline silver-copper sulphide (jalpaite, Ag_3CuS_2); Type 4 niello is inhomogeneous silver-copper sulphide (exsolution of jalpaite, Ag_3CuS_2 and mckinstryite, $Ag_5Cu_3S_4$); and Type 5 niello is homogeneous polycrystalline silver-copper sulphide (stromeyerite, AgCuS) (**Figs. 4-5.**) (Mozgai et al. 2019).

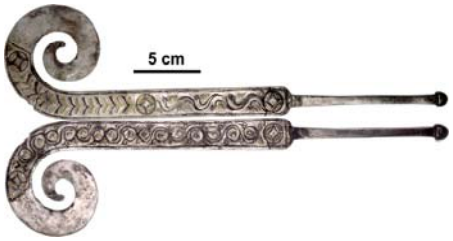

Fig. 3.: The late Roman silver augur staff (*lituus*) decorated with niello inlays (photo: A. Dabasi, Hungarian National Museum)

3. ábra: A niellóberakásokkal díszített késő római ezüst augurbot (*lituus*) (fotó: Dabasi A., Magyar Nemzeti Múzeum)

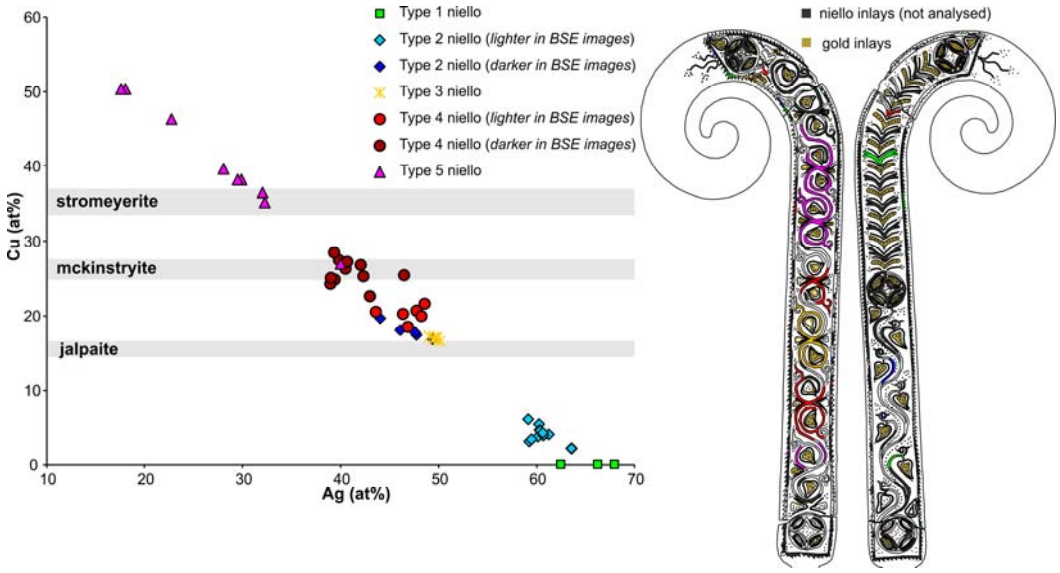

Fig. 4.: Chemical composition of the different niello types of the augur staff based on SEM-EDS measurements and the distribution of different types of niello inlays on the augur staff based on the SEM-EDS and μ-XRD results. Chemical ranges for silver-copper sulphides are based on Grybeck & Finney (1968) for jalpaite ($Ag_{1.55}Cu_{0.45}S$–$Ag_{1.5}Cu_{0.5}S$); Skinner et al. (1966) and Kolitsch (2010) for mckinstryite ($Ag_{1.18}Cu_{0.82}S$–$Ag_{1.25}Cu_{0.75}S$) and Frueh (1955) and Tokuhara et al. (2009) for stromeyerite ($Ag_{0.9}Cu_{1.1}S$–$Ag_{1.0}Cu_{1.0}S$), respectively. Note that Type 5 niello exhibits higher copper concentrations than ideal stromeyerite due to the presence of surface corrosion products.

4. ábra: A különböző niellótípusok kémiai összetétele a SEM-EDS elemzések alapján és a különböző niellótípusok eloszlása az augurboton a SEM-EDS és μ-XRD eredmények alapján. Az ezüst-réz-szulfidok kémiai tartománya: jalpait ($Ag_{1,55}Cu_{0,45}S$–$Ag_{1,5}Cu_{0,5}S$) Grybeck & Finney (1968) alapján; mckinstryit ($Ag_{1,18}Cu_{0,82}S$–$Ag_{1,25}Cu_{0,75}S$) Skinner et al. (1966) és Kolitsch (2010) alapján és stromeyerit ($Ag_{0,9}Cu_{1,1}S$–$Ag_{1,0}Cu_{1,0}S$) Frueh (1955) és Tokuhara et al. (2009) alapján. Az 5. típusú niellóban az ideális stromeyeritnél nagyobb réztartalom oka a felületen jelenlevő korróziós termékek.

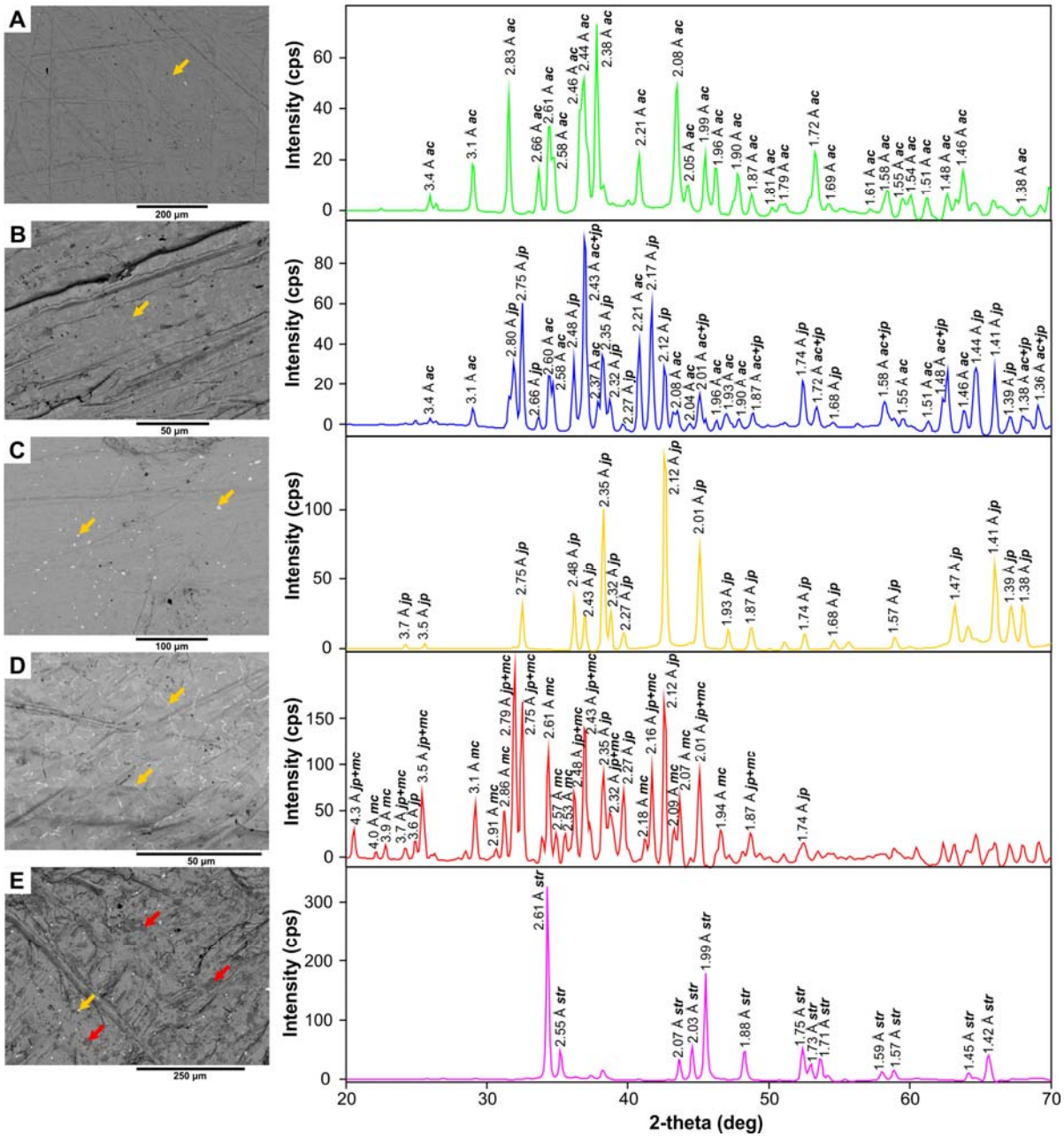

Fig. 5.: Back-scattered electron (BSE) images and µ-XRD patterns of the niello types. A: Type 1 – homogeneous silver sulphide (acanthite); B: Type 2 – inhomogeneous silver-copper sulphide (exsolution of acanthite and jalpaite); C: Type 3 – homogeneous silver-copper sulphide (jalpaite); D: Type 4 – inhomogeneous silver-copper sulphide (exsolution of jalpaite and mckinstryite); E: Type 5 – homogeneous silver-copper sulphide (stromeyerite), darker phases are copper- and iron-containing surface patches (red arrows). Metallic gold is accumulated along the grain boundaries in each type of niello forming bright inclusions and strings in BSE images (yellow arrows). Abbreviations: ac = acanthite (Ag_2S) (PDF 00-014-0072); jp = jalpaite (Ag_3CuS_2) (PDF 00-012-0207); mc = mckinstryite ($Ag_5Cu_3S_4$) (PDF 00-019-0406); str = stromeyerite (AgCuS) (PDF 00-012-0156).

5. ábra: A különböző niellótípusok visszaszórtelektron-képei (BSE) és diffraktogramjai. A: 1. típus – homogén ezüst-szulfid (akantit); B: 2. típus – inhomogén ezüst-réz-szulfid (akantit és jalpait szételegyedése); C: 3. típus – homogén ezüst-réz-szulfid (jalpait); D: 4. típus – inhomogén ezüst-réz-szulfid (jalpait és mckinstryit szételegyedése); E: 5. típus – homogén ezüst-réz-szulfid (stromeyerit), a sötétebb fázisok réz- és vastartalmú felületi kiválások (piros nyilak). Az arany mindegyik niellótípusban a szemcsehatárok mentén vált ki, a BSE képeken világos zárványok formájában (sárga nyilak). Rövidítések: ac = akantit (Ag_2S) (PDF 00-014-0072); jp = jalpait (Ag_3CuS_2) (PDF 00-012-0207); mc = mckinstryit ($Ag_5Cu_3S_4$) (PDF 00-019-0406); str = stromeyerit (AgCuS) (PDF 00-012-0156).

The augur staff decorated with such heterogeneous niello inlays is the first object ever analysed in this manner. Based on archaeological arguments the augur staff is well-dated to 260–280s AD and was presumably buried with the last augur of *Brigetio* in the early decades of the 4th century AD (Barkóczi 1965; Mráv 2010a; 2010b). Both mineralogical and archaeological arguments link niello heterogeneity to the primary production of the object rather than to any post-production repair or post-burial corrosion processes (Mozgai et al. 2019). The variable copper content of the niello decorations of the augur staff indicates no technological innovation. The silversmith simply employed not only silver but in order to make up for the shortage of silver also differently debased silver, possibly scrap materials of the workshop for producing niello (Mozgai et al. 2019). The elevated copper content of niello inlays shows that silver-copper sulphide niello, even stromeyerite (AgCuS), was used by the Roman craftsmen two-hundred years earlier (last third of 3rd century AD) than the previous studies indicated (end of 5th century AD).

Case study 2: Corrosion products of a late Roman copper cauldron

Corrosion products of a large-sized late Roman copper cauldron (**Fig. 6.**), with uncertain provenance (finding location) and now stored in the Hungarian National Museum, were examined. The cauldron is part of the Seuso Treasure, and fourteen large silver vessels were hidden in it; the imprints of the rim of the platters were detected on the inner side of the cauldron (Nagy & Tóth 1990; Bennett 1994; Nagy 2012; Visy 2012). The object is rather large-sized: 83 cm in diameter and 32.5 cm in height, 150 litres capacity. This cylindrical cauldron with an originally convex bottom has stepped wall made of two separate hammered copper sheets joined together with hammering, riveting and soldering. The wall is joined to the bottom with crenelated seam. The cauldron was most probably manufactured in the 3rd or 4th century AD. Based on its shape and manufacturing techniques, it belongs to a type widespread in the Rhine and Danube regions of the Roman Empire in the 2nd–4th centuries AD. The southernmost examples of this type of object were unearthed in the Transdanubian region of Pannonia around Lake Balaton in Hungary (Nagy & Tóth 1990; Nagy 2012).

Fig. 6.: Late Roman copper cauldron (photo: A. Dabasi, Hungarian National Museum) and one of the corroded metal samples taken from the cauldron.

6. ábra: Késő római rézüst (fotó: Dabasi A., Magyar Nemzeti Múzeum) és az üstből kivett, korrodált fémminták egyike.

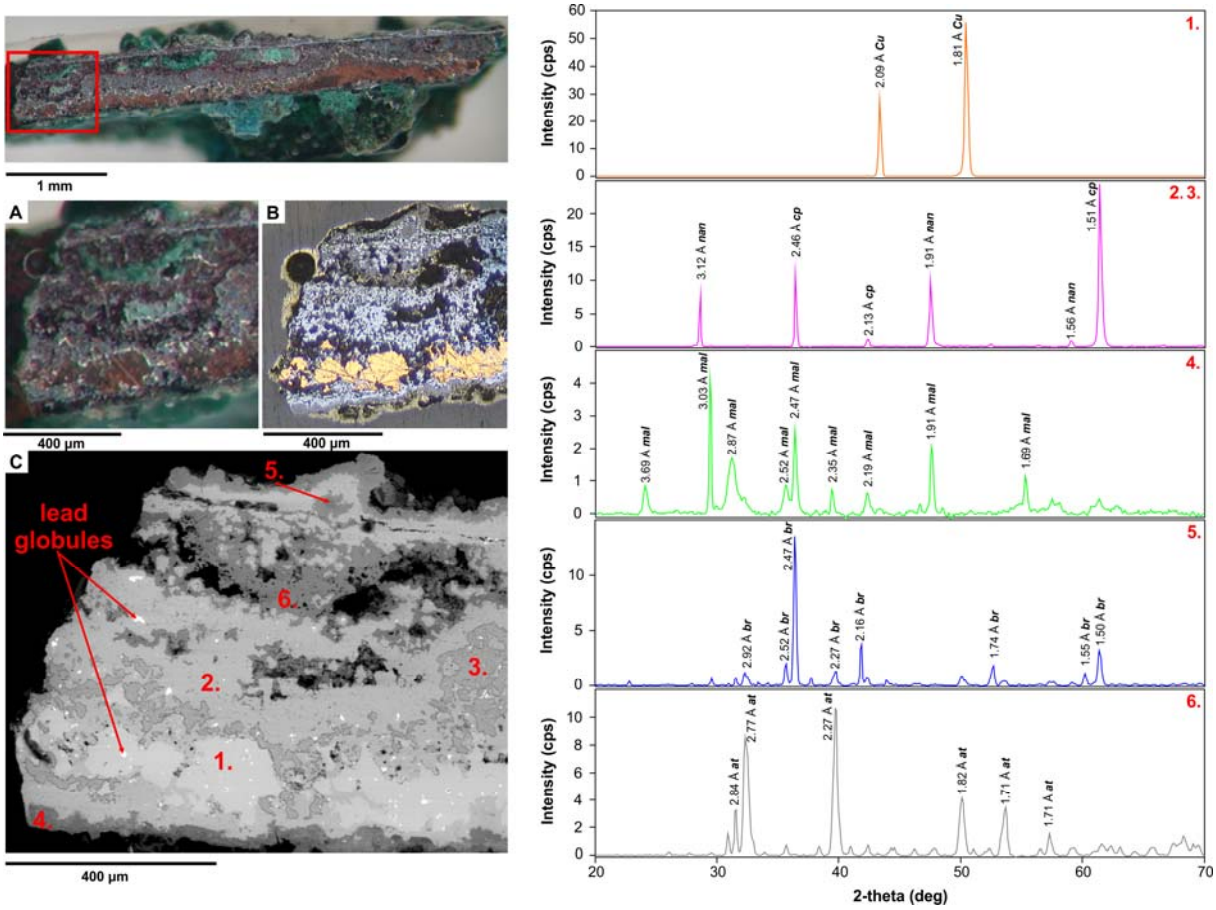

Fig. 7.: Binocular (A), reflected light microscopy (B) and back-scattered electron (BSE) (C) images of the cross section of a small corroded metal sample detached from the cauldron. Bright patches in BSE image are lead globules dispersed in the metal. µ-XRD patterns of the layers of the corroded metal: 1. uncorroded copper, 2. copper oxide (cuprite), 3. copper chloride (nantokite), 4. copper carbonate (malachite), 5. copper sulphate (brochantite), 6. copper hydroxychloride (atacamite/paratacamite). Abbreviations: Cu = copper metal (PDF 01-085-1326); cp = cuprite (Cu_2O) (PDF 01-078-2076); nan = nantokite (CuCl) (PDF 00-006-0344); mal = malachite ($Cu_2CO_3(OH)_2$) (PDF 01-076-0660); br = brochantite ($Cu_4SO_4(OH)_6$) (PDF 01-087-0454); at = atacamite/paratacamite ($Cu_2Cl(OH)_3$) (PDF 01-077-0116).

7. ábra: Az üstből levett korrodált fémminta keresztmetszetének sztereomikroszkópos (A), ráesőfényes polarizációs mikroszkópos (B) és visszaszórtelektron-képe (C). Az ólom világos zárványok formájában elkülönült a réztől. A különböző korróziós rétegek diffraktogramjai: 1. vörösréz, 2. réz-oxid (kuprit), 3. réz-klorid (nantokit), 4. réz-karbonát (malachit), 5. réz-szulfát (brochantit), 6. réz-hidroklorid (atacamit/paratacamit). Rövidítések: Cu = vörösréz (PDF 01-085-1326); cp = kuprit (Cu_2O) (PDF 01-078-2076); nan = nantokit (CuCl) (PDF 00-006-0344); mal = malachit ($Cu_2CO_3(OH)_2$) (PDF 01-076-0660); br = brochantit ($Cu_4SO_4(OH)_6$) (PDF 01-087-0454); at = atacamit/paratacamit ($Cu_2Cl(OH)_3$) (PDF 01-077-0116).

The appearance of the cauldron, the extent of corrosion, and its overall preservation state indicates that it was kept in a protected environment. Thick calcareous encrustations and soil remnants on the surface implies that the cauldron was probably buried in soil for a long time. Our aim was to determine and characterise the burial environment and the corrosion processes with the characterisation of the different corrosion products found on the cauldron, since they may hold clues about the burial conditions (Eh, pH, etc.) of the object.

An *in situ*, layer-by-layer analysis was performed on polished cross sections of small corroded metal samples detached from the cauldron by using EPMA and µ-XRD (**Fig. 1c**). Only the latter method enables to determine the mineralogical composition of the different corrosion products forming layers separately. The cauldron is made of unalloyed copper, small (few micrometer-sized) lead globules are dispersed in the metal. Two corrosion zones are present: (1) the original (internal) surface zone of the metallic copper was replaced by copper oxide (cuprite, Cu_2O), whereas (2) basic copper carbonate (malachite,

$Cu_2CO_3(OH)_2$) was deposited (externally) on the original surface along with calcium carbonate (calcite, $CaCO_3$) incorporating some soil minerals (e.g. quartz, feldspars) (**Fig. 7.**). These copper minerals were formed during long-time burial (passive corrosion) and protected the cauldron from further severe corrosion, therefore, their appearance corresponds well with a well-aerated, calcareous soil burial environment with moderate pH and Eh (**Fig. 8.**) (Tylecote 1979; Miller et al. 1981; McNeil & Little 1992; Schweizer 1994; Scott 2002). Based on the absence of copper sulphides, anoxic and waterlogged environment as burial site can be excluded (Tylecote 1979; Miller et al. 1981; McNeil & Little 1992; Schweizer 1994; Scott 2002). Rarely copper chloride (nantokite, CuCl), basic copper trihydroxychloride (paratacamite / atacamite, $Cu_2Cl(OH)_3$) and basic copper sulphate (brochantite, $Cu_4SO_4(OH)_6$) were also identified in the two corrosion zones (**Fig. 7.**). Their uneven distribution on the cauldron and their formation conditions (typically formed on air, in outdoor environments, not in soil environments) indicate that these minerals may be the results of active corrosion, forming most possibly after excavation (**Fig. 8.**) (Tylecote 1979; Scott 2002).

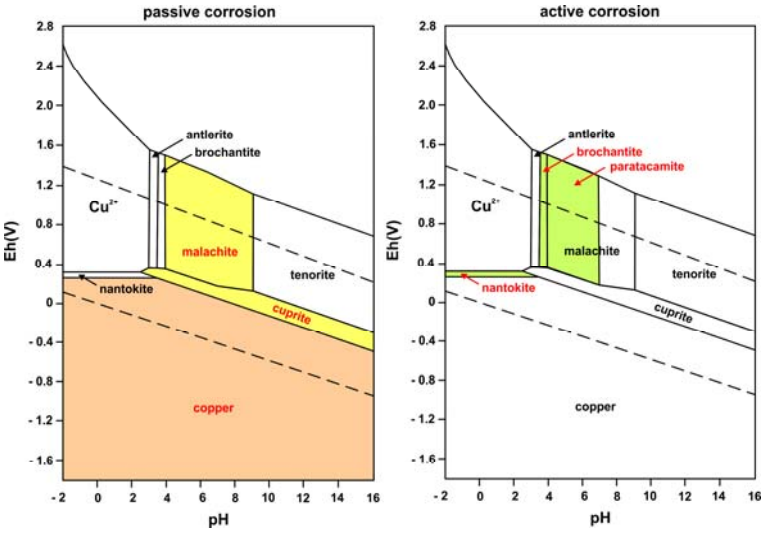

Fig. 8.: Pourbaix diagrams of the Cu–CO_3–SO_4–Cl–H_2O system indicating the stability field of the different copper corrosion products for solutions containing 229 ppm CO_2 and 46 ppm SO_3 (after Pourbaix 1977). Passive corrosion products (cuprite, malachite) were formed in moderate pH and Eh conditions, whereas active corrosion products (nantokite, paratacamite/atacamite, brochantite) indicate a more oxidative and/or acidic environment.

8. ábra: A különböző rézkorróziós termékek stabilitási mezeje a Cu–CO_3–SO_4–Cl–H_2O rendszer Pourbaix diagramjain (229 ppm CO_2, 46 ppm SO_3) (Pourbaix 1977 nyomán). A passzív korróziós termékek (kuprit, malachit) közepes Eh-pH viszonyok közt keletkeztek, míg az aktív korrózió termékei (nantokit, paratacamit/atacamit, brochantit) savasabb és/vagy oxidatívabb környezetet jelölnek.

Case study 3: Corrosion products of Hunnic-period gold and gilded silver objects

A lonely grave (SNR 2785) of an 18–20-year-old man was discovered during the preventive excavation of the expansion of the Mercedes factory in Kecskemét-Mindszenti-dűlő in 2017. Based on the attire items (gold hair ring, knife with a gold sheat-decorated handle, different buckles covered with gold foil) and the sword buried with the deceased, the grave can be dated to the Hunnic period. The sword also indicates his high social status, who supposed to be a noble member of the society. Both the finds and the rite of this burial differs from the traditions of the Sarmatians, who lived in this area during this period. This may prove that after the arrival of the Huns into the Carpathian Basin, they chose one of their nobility to be the leader of the Sarmatians, who lived this area of the Danube-Tisza Interfluve for hundreds of years. The deceased can be this nobility or one of his relatives.

Fig. 9.: The analysed objects from Kecskemét–Mindszenti-dűlő: a gold hair ring, a ribbed gold sheet and four gilded silver buckles (photo: B. Kiss, Katona József Museum of Kecskemét).

9. ábra: Kecskemét–Mindszenti-dűlőn előkerült és elemzett tárgyak: arany hajkarika, bordázott aranylemez és négy aranyozott ezüstcsat (fotó: Kiss B., Kecskeméti Katona József Múzeum).

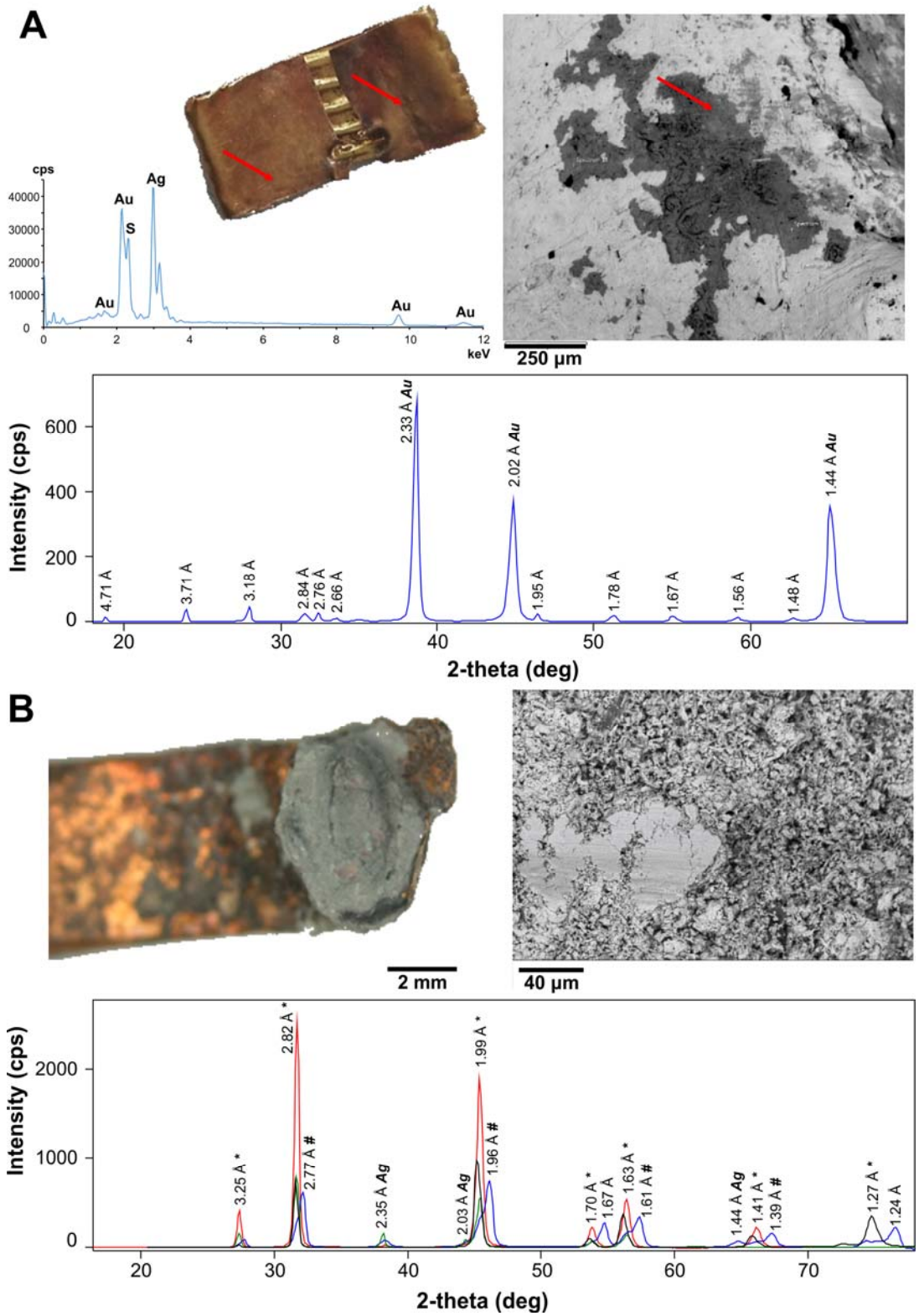

Fig. 10.: A: Macroscopic and back-scattered electron (BSE) images, energy-dispersive X-ray spectrum and µ-XRD pattern of the thin reddish layer (red arrows) on the surface of the ribbed gold sheet. B: Binocular microscopic and back-scattered electron (BSE) images and µ-XRD patterns of the corroded silver alloy of the buckles. Symbols and abbreviations: Au = gold (JCPDS 04-0784); Ag = silver (JCPDS 87-0720); *: Ag(Cl,Br) (JCPDS 14-0255); #: Ag_3SBr (JCPDS 18-1189).

10. ábra: A: A bordázott aranylemez felületén megjelenő vékony, vöröses színű réteg (piros nyilak) makroszkópos és visszaszórtelektron-képe (BSE), energiadiszperzív röntgenspektruma és diffraktogramja. B: A korrodált ezüstcsatok sztereomikroszkópos és visszaszórtelektron-képe, és µ-XRD diffraktogramjai. Szimbólumok és rövidítések: Au = arany (JCPDS 04-0784); Ag = ezüst (JCPDS 87-0720); *: Ag(Cl,Br) (JCPDS 14-0255); #: Ag_3SBr (JCPDS 18-1189).

The material and the corrosion products of gold and gilded silver objects, namely a gold hair ring, a ribbed gold sheet and four gilded silver buckles found in the grave (**Fig. 9.**), were analysed non-destructively by using EPMA and μ-XRD (**Fig. 1d**). The silver objects are heavily corroded; therefore, the original composition of the used alloy can barely be determined.

The gold hair ring and the ribbed gold sheet were both manufactured from a high-quality gold alloy (gold hair ring (n=4): 91.9±2.4 wt% Au, 6.0±1.2 wt% Ag, 0.7±0.1 wt% Cu; ribbed gold sheet (n=4): 96.1±2.8 wt% Au, 3.4±0.2 wt% Ag, 0.6±0.3 wt% Cu, 0.2±0.1 wt% Fe). The surface of the ribbed gold sheet is covered with a very thin reddish layer (**Fig. 10a**). The reddish coloration of gold objects is a well-known and studied phenomena, and can be related to (1) addition of red materials onto the surface (coating with cinnabar (HgS) or with iron oxides) (Shimada & Griffin 2005; Rastrelli et al. 2009), (2) specific composition of alloy (gold alloys with high copper content) (Lucas 1962; Troalen et al. 2009), or (3) surface corrosion (presence of silver-gold sulphides, e.g. petrovskaite (AgAuS), uytenbogaardtite (Ag_3AuS_2), in addition, acanthite (Ag_2S), silver sulphate (Ag_2SO_4) and chalcocite (Cu_2S)) (Lucas 1962; Frantz & Schorsch 1990; Randin et al. 1992; Gusmano et al. 2004; Selwyn 2004; Griesser et al. 2005; Mayerhofer et al. 2005; Bastidas et al. 2008; Tissot et al. 2009; Liang et al. 2011; Guerra & Tissot 2013; Tissot et al. 2015). It is difficult to identify the mineralogical composition of the corrosion tarnish, due to its few hundred Å thickness (Ankersmit et al. 2005; Bastidas et al. 2008; Guerra & Tissot 2013). Based on the EPMA and μ-XRD measurements, the reddish layer is a tarnish most probably composed of the mixtures of gold-silver sulphides (and other corrosion products) (**Fig. 10a**). Since the tarnish layer is very thin and μ-XRD intensities are not relevant, we could not determine its exact mineralogical composition merely taking into consideration the peak positions.

The buckles were manufactured from a silver alloy covered with approx. 0.05–0.1 mm thick gold foil ('foil-gilding'). The gold foils were produced from high-quality gold: three of the buckles were decorated with foils of 94.8–96.4 wt% gold content, whereas one of the buckles was covered with leaf of 88.0 wt% gold content. The original silver alloy has completely mineralised during corrosion processes (**Fig. 10b**). The EPMA and μ-XRD measurements proved the presence of silver, sulphur, chloride and bromide in the form of silver sulphobromide (Ag_3SBr) and bromian chlorargyrite (embolite, Ag(Cl,Br)) (**Fig. 10b**). Copper corrosion products were not determined; therefore, the objects were most probably manufactured from a high-purity silver alloy. The silver sulphides and chlorides are the typical corrosion products of silver objects buried in soils, whereas silver bromides are characteristic only of soils with high organic matter content (Hedges 1976; McNeil & Little 1992; Martina et al. 2012; Marchand et al. 2014). The presence of silver chloride indicates shallow burial in soil (McNeil & Little 1992).

Acknowledgements

The authors are thankful to Balázs Lencz and Tamás Szabadváry (Hungarian National Museum), Máté Szabó (Institute for Geological and Geochemical Research, RCAES, HAS), Péter Németh (Institute for Materials and Environmental Chemistry, RCNS, HAS), Boglárka A. Topa (Department of Mineralogy and Petrology, Hungarian Natural History Museum) and Tamás Weiszburg (Department of Mineralogy, Eötvös Loránd University) for their help in sampling, measurement and data evaluation.

References

ABBE, M. B., BORROMEO, G. E. & PIKE, S. A. (2012): Hellenistic Greek marble statue with ancient polychromy reported to be from Knidos. In: GUTIÉRREZ GARCIA M.A., LAPUENTE MERCADAL, P. & RODÀ DE LLANZA, I. (eds.): *Interdisciplinary Studies on Ancient Stone. Proceedings of the IX Association for the Study of Marbles and Other Stones in Antiquity (ASMOSIA) Conference (Tarragona 2009).* Institut Català d'Arqueologia Clàssica, Tarragona. 763–770.

ANKERSMIT, H. A., TENNENT, N. H. & WATTS, S. F. (2005): Hydrogen sulfide and carbonyl sulfide in the museum environment – Part 1. *Atmospheric Environment* **39** 695–707.

BAJNÓCZI, B., SZABÓ, M. & TÓTH, M. (2016): Technological studies of historical glazes with the use of RIGAKU D/MAX RAPID II micro-XRD. In: CARMINA, B. & PASERO, M. (eds.): *2nd Mineralogical Conference, 11–15 September 2016, Rimini, Italy,* Book of abstracts, Rimini, p. 704.

BARKÓCZI, L. (1965): New data on the history of Late Roman Brigetio. *Acta Antiqua Academiae Scientiarum Hungaricae* **13** 215–257.

BASTIDAS, D. M., CANO, E., GONZÁLEZ, A. G., FAJARDO, S., LLERAS-PÉREZ, R., CAMPO-MONTERO, E., BELZUNCE-VARELA, F. J. & BASTIDAS, J. M. (2008): XPS study of tarnishing of a gold mask from a pre-Columbian culture. *Corrosion Science* **50** 1785–1788.

BENEDETTI, D., VALETTI, S., BONTEMPI, E., PICCIOLI, C. & DEPERO, L. E. (2004): Study of ancient mortars from the Roman Villa of Pollio Felice in Sorrento (Naples). *Applied Physics A: Materials Science & Processing* **79** 341–345.

BENNETT, A. (1994): Technical examination and conservation. In: MANGO, M. M. & BENNETT, A.: The Sevso Treasure. *Journal of Roman Archaeology Supplementary Series* **12** Ann Arbor, MI, 21–37.

BONTEMPI, E., BENEDETTI, D., MASSARDI, A., ZACCO, A., BORGESE, L. & DEPERO, L. E. (2008): Laboratory two-dimensional X-ray microdiffraction technique: a support for authentication of an unknown Ghirlandaio painting. *Applied Physics A: Materials Science & Processing* **92** 155–159.

DENNIS, J. R. (1979): Niello: a technological study. In: *Papers presented by trainees at the Art Conservation training programs conference. The Cricket Press, Manchester, Massachusetts*, 83–95.

FRANTZ, J. H. & SCHORSCH, D. (1990): Egyptian Red Gold. *Archeomaterials* **4** 133–152.

FRUEH, A. J. (1955): The crystal structure of stromeyerite, AgCuS: A possible defect structure. *Zeitschrift für Kristallographie* **106** 299–307.

GRIESSER, M., TRAUM, R., MAYERHOFER, K., PIPLITS, K., DENK, R. & WINTER, H. (2005): Brown spot corrosion on historic gold coins and medals. *Surface Engineering* **21** 385–392.

GRYBECK, D. & FINNEY, J. J. (1968): New occurrences and data for jalpaite. *The American Mineralogist* **53** 1530–1542.

GUERRA, M. F. & TISSOT, I. (2013): The role of nuclear microprobes in the study of technology, provenance and corrosion of cultural heritage: The case of gold and silver items. *Nuclear Instruments and Methods in Physics Research B* **306** 227–231.

GUSMANO, G., MONTANARI, R., MONTESPERELLI, S. & DENK, R. (2004): Gold corrosion: red stains on a gold Austrian Ducat. *Applied Physics A* **79** 205–211.

HEDGES, R. E. M. (1976): On the occurrence of bromine in corroded silver. *Studies in Conservation* **21/1** 44–46.

HOWE, E., KAPLAN, E., NEWMAN, R., FRANTZ, J. H., PEARLSTEIN, E., LEVINSON, J. & MADDEN, O. (2018): The occurrence of a titanium dioxide/silica white pigment on wooden Andean qeros: a cultural and chronological marker. *Heritage Science* **6/41** 1–12.

KINGERY-SCHWARTZ, A., POPELKA-FILCOFF, R. S., LOPEZ, D. A., POTTIER, F., HILL, P. & GLASCOCK, M. (2013): Analysis of geological ochre: its geochemistry, use, and exchange in the US Northern Great Plains. *Open Journal of Archaeometry* **1(e15)** 72–76.

KOLITSCH, U. (2010): The crystal structure and compositional range of mckinstryite. *Mineralogical Magazine* **74/1** 73–84.

LA NIECE, S. (1983) Niello: an historical and technical survey. *The Antiquaries Journal* **58/2** 279–297.

LIANG, C., YANG, C. & HUANG, N. (2011): Investigating the tarnish and corrosion mechanisms of Chinese gold coins. *Surface and Interface Analysis* **43** 763–769.

LUCAS, A. (1962): *Ancient Egyptian Materials and Industries.* Edward Arnold & Co., London, pp. 584.

MARCHAND, G., GUILMINOT, E., LEMOINE, S., ROSSETTI, L., VIEAU, M. & STEPHANT, N. (2014): Degradation of archaeological horn silver artefacts in burials. *Heritage Science* **2/5** 1–7.

MARTINA, I., WIESINGER, R., JEMBRIH-SIMBÜRGER, D. & SCHREINER, M. (2012): Micro-Raman characterisation of silver corrosion products: instrumental set up and reference database. *e-PRESERVATION Science*, **9** 1–8.

MAYERHOFER, K., PIPLITS, K., TRAUM, R., GRIESSER, M. & HUTTER, H. (2005): Investigation of corrosion phenomena on gold coins with SIMS. *Applied Surface Science* **252** 133–138.

MCNEIL, M. B. & LITTLE, B. J. (1992): Corrosion mechanisms for copper and silver objects in near-surface environments. *Journal of the American Institute for Conservation* **31/3** 355–366.

MILLER, F. P., FOSS, J. E. & WOLF, D. C. (1981): Soil surveys: their synthesis, confidence limits and utilization for corrosion assessment of soil. In: ESCALANTE, E. (ed.): *Underground Corrosion. American Society for Testing and Materials Special Technical Publication* **741**. Philadelphia: ASTM. 3–23.

MOSS, A. A. (1953) Niello. *Studies in Conservation* **1/2** 49–62.

MOZGAI, V., FÓRIZS, I., BAJNÓCZI, B., CSEDREKI, L., KERTÉSZ, ZS., MAY, Z., SZABÓ, M., MRÁV, ZS. & TÓTH, M. (2016): Analysis of niello inlay in Roman silver- and copper-based alloy metalwork found in the Pannonian provinces. In: ZACHARIAS, N. & PALAMARA, E. (eds.): *41st International Symposium on Archaeometry (ISA 2016)* Book of Abstracts 15–20 May 2016 Kalamata, Greece, University of Peloponnese, Kalamata, 122–123.

MOZGAI, V., TOPA, B. A., WEISZBURG, T. G., MRÁV, ZS. & BAJNÓCZI, B. (2019): SEM–EDS and μ-XRD study of the niello inlays of a unique late Roman silver augur staff (*lituus*) from Brigetio, Pannonia (Hungary). *Archaeological and Anthropological Sciences* **11** 1599–1610.

MRÁV, ZS. (2010a): Roman trifid phalera pendant with metal inlay decoration from Biatorbágy (Pest County, Hungary) / Fémberakással díszített kora császárkori phaleracsüngő Biatorbágyról. In: KVASSAY, J. (ed.): *Field Service for Cultural Heritage 2008 Yearbook and Review of Archaeological Investigations*, Kulturális Örökség-védelmi Szakszolgálat, Budapest, 139–161.

MRÁV, ZS. (2010b): Egy késő 3. századi, niellóberakással díszített középgyűrűs bronz szíjvégveret Brigetióból [A late third-century niello-inlaid strap terminal from Brigetio]. *Komárom-Esztergom Megyei Múzeumok Közleményei* **16** 13–40.

MRÁV, ZS. (2011): Egy késő 3. századi niellóberakásos bronz övlemez töredéke a Magyar Nemzeti Múzeumban – előzetes közlés [Fragment of a late third-century niello-inlay belt mounting at the Hungarian National Museum. A preliminary report]. In: TÓTH, E. & VIDA, I. (eds.): *Corolla Museologica Tibor Kovacs Dedicata,* Hungarian National Museum, Budapest, 365–402.

NAGY, M. & TÓTH, E. (1990): The Seuso Treasure. The Pannonian connection? *Minerva* **1/7** 4–11.

NAGY, M. (2012): A Seuso-kincs pannoniai kapcsolatai [Connections of the Seuso Treasure to Pannonia]. In: VISY, ZS. & MRÁV, ZS. (eds.): *A Seuso-kincs és Pannonia [The Sevso Treasure and Pannonia],* PTE Régészeti Tanszék – GeniaNet, Pécs, 49–63.

NEWMAN, R., DENNIS, J. R. & FARREL, E. (1982): A technical note on niello. *Journal of the American Institute for Conservation* **21/2** 80–85.

NORTHOVER, P. & LA NIECE, S. (2009): New thoughts on niello. In: SHORTLAND, A. I., FREESTONE, I. & REHREN, T. (eds.): *From Mine to Microscope: Advances in the Study of Ancient Technology,* Oxbow Books, Oxford, 145–154.

ODDY, W. A., BIMSON, M. & LA NIECE, S. (1983): The composition of niello decoration on gold, silver and bronze in the antique and mediaeval periods. *Studies in Conservation* **28/1** 29–35.

OSVÁTH, ZS., FÓRIZS, I., SZABÓ, M. & BAJNÓCZI, B. (2018): Archaeometric analysis of some Scythian and Celtic glass beads from Hungary. *Archeometriai Műhely* **15/1** 29–44.

POURBAIX, M. (1977): Electrochemical Corrosion and Reduction, Corrosion and Metal Artifacts. In: BROWN, B. F., BURNETT, H. C., CHASE, W. T., GOODWAY, M., KRUGER, J. & POURBAIX, M. (eds.): A *Dialogue Between Conservators and Archaeologists and Corrosion Scientists. NBS Special Publication,* no. **479**. Washington, D.C.: National Bureau of Standards, 1–16.

RANDIN, J. P., RAMONI, P. & RENAUD, J. P. (1992): Tarnishing of AuAgCu alloys. Effect of the composition. *Werkstoffe und Korrosion* **43** 115–123.

RASTRELLI, A., MICCIO, M., MARTINÓN-TORRES, M., GUERRA, M. F., SIANO, S. & VITOBELLO, M. L. (2009): Modern and ancient gold jewellery attributed to the Etruscans: a science-based study. *ArchéoSciences* **33** 357–364.

SCHWEIZER, F. (1993): Nielle byzantine: étude de son evolution. *Geneva* **41** 67–82.

SCHWEIZER, F. (1994): Bronze objects from lake sites: from patina to "biography". In: SCOTT, D. A., PODANY, J. & CONSIDINE, B. B. (eds.): *Ancient & Historic Metals: Conservation and Scientific Research.* The Getty Conservation Institute. 33–50.

SCOTT, D. A. (2002): *Copper and Bronze in Art – Corrosion, colorants, conservation.* Getty Publications, Los Angeles; pp. 515.

SELWYN, L. (2004): *Metals and Corrosion. A Handbook for the Conservation Professional.* Canadian Conservation Institute, Ottawa, pp. 223.

SHIMADA, I. & GRIFFIN, J. A. (2005): Precious metal objects of the middle Sicán. *Scientific American* **15/1** 80–89.

SKINNER, B. J., JAMBOR, J. L. & ROSS, M. (1966): Mckinstryite, a new copper-silver sulfide. *Economic Geology* **61/8** 1383–1389.

SWIDER, J. R. (2010): Powder micro-XRD of small particles. *Powder Diffraction* **25/1** 68–71.

TAKUMI, Y. & MAEYAMA, M. (2015): Micro X-ray diffraction of cultural properties. *Rigaku Journal* **31/2** 1–11.

TISSOT, I., TISSOT, M., PEDROSO, P. & RAPOSO, L. (2009): Treasures of Portuguese archaeology. Notes towards a preventive conservation project. *ArchéoSciences* **33** 389–392.

TISSOT, I., TROALEN, L. G., MANSO, M., PONTING, M., RADTKE, M., REINHOLZ, U., BARREIROS, M. A., SHAW, I., CARVALHO, M. L. & GUERRA, M. F. (2015): A multi-analytical approach to gold in Ancient Egypt: Studies on provenance and corrosion. *Spectrochimica Acta Part B* **108** 75–82.

TOKUHARA, Y., TEZUKA, K., SHAN, Y. J. & IMOTO, H. (2009): Syntheses of complex sulfides AgCuS and Ag_3CuS_2 from the elements under hydrothermal conditions. *Journal of the Ceramic Society of Japan* **117/3** 359–362.

TÓTH, E. (2017): Augurenstab aus Komárom. In: LÜBKE, CH. & HARDT, M. (eds.): *Vom spätantiken Erbe zu den Anfangen der Romanik: 400–1000. Handbuch zur Geschichte der Kunst in Ostmitteleuropa* Bd. 1. Deutscher Kunstverlag, Leipzig, 280–281.

TROALEN, L., GUERRA, M. F., TATE, J. & MANLEY, B. (2009): Technological study of gold jewellery pieces dating from the Middle Kingdom to the New Kingdom in Egypt. *ArchéoSciences* **33** 111–120.

TYLECOTE, R. F. (1979): The effect of soil conditions on the long-term corrosion of buried tin-bronzes and copper. *Journal of Archaeological Science* **6** 345–368.

VISY, Zs. (2012): A Seuso-kincs ismert darabjai [The known objects of the Seuso treasure]. In: VISY, ZS. & MRÁV, ZS. (eds.): *A Seuso-kincs és Pannonia [The Sevso Treasure and Pannonia],* PTE Régészeti Tanszék – GeniaNet, Pécs, 7–22.

HU ISSN 1786-271X; urn: nbn: hu-4106 © by the author(s)